Biosensors and Bioelectronics 253 (2024) 116166

Contents lists available at ScienceDirect

Biosensors and Bioelectronics

journal homepage: www.elsevier.com/locate/bios

A skin-interfaced, miniaturized platform for triggered induction, capture and colorimetric multicomponent analysis of microliter volumes of sweat

Joohee Kim [a,b,c,1], Seyong Oh [b,d,1], Da Som Yang [b,1], Larissa Rugg [e], Radhika Mathur [e], Sung Soo Kwak [a,b], Seonggwang Yoo [b], Shupeng Li [g], Evangelos E. Kanatzidis [b], Geumbee Lee [b], Hong-Joon Yoon [b,f], Yonggang Huang [b,g], Roozbeh Ghaffari [b,h,i], Susanna A. McColley [e,j,*], John A. Rogers [b,g,h,i,k,l,**]

[a] Center for Bionics of Biomedical Research Division, Korea Institute of Science and Technology, Seoul, 02792, Republic of Korea
[b] Querrey Simpson Institute for Bioelectronics, Northwestern University, Evanston, IL, 60208, USA
[c] Precision Biology Research Center, Sungkyunkwan University, Suwon, 16419, Republic of Korea
[d] Division of Electrical Engineering, Hanyang University ERICA, Ansan, 15588, Republic of Korea
[e] Division of Pulmonary and Sleep Medicine, Ann & Robert H. Lurie Children's Hospital of Chicago, Chicago, IL, 60611, USA
[f] Department of Electronic Engineering, Gachon University, Seongnam-si, Gyeonggi-do 13120, Republic of Korea
[g] Department of Mechanical Engineering, Northwestern University, Evanston, IL, 60208, USA
[h] Department of Biomedical Engineering, Northwestern University, Evanston, IL, 60208, USA
[i] Epicore Biosystems Inc., Cambridge, MA, 02139, USA
[j] Department of Pediatrics, Feinberg School of Medicine, Northwestern University, Chicago, IL, 60611, USA
[k] Department of Materials Science and Engineering, Northwestern University, Evanston, IL, 60208, USA
[l] Department of Neurological Surgery, Feinberg School of Medicine, Northwestern University, Chicago, IL, 60611, USA

ARTICLE INFO

Keywords:
Bioelectronics
Sweat induction
Sweat collection
Health monitoring

ABSTRACT

Eccrine sweat can serve as a source of biomarkers for assessing physiological health and nutritional balance, for tracking loss of essential species from the body and for evaluating exposure to hazardous substances. The growing interest in this relatively underexplored class of biofluid arises in part from its non-invasive ability for capture and analysis. The simplest devices, and the only ones that are commercially available, exploit soft microfluidic constructs and colorimetric assays with purely passive modes of operation. The most sophisticated platforms exploit batteries, electronic components and radio hardware for inducing sweat, for electrochemical evaluation of its content and for wireless transmission of this information. The work reported here introduces a technology that combines the advantages of these two different approaches, in the form of a cost-effective, easy-to-use device that supports on-demand evaluation of multiple biomarkers in sweat. This flexible, skin-interfaced, miniaturized system incorporates a hydrogel that contains an approved drug to activate eccrine sweat glands, electrodes and a simple circuit and battery to delivery this drug by iontophoresis through the surface of the skin, microfluidic channels and microreservoirs to capture the induced sweat, and multiple colorimetric assays to evaluate the concentrations of chloride, zinc, and iron. As demonstrated in healthy human participants monitored before and after a meal, such devices yield results that match those of traditional laboratory analysis techniques. Clinical studies that involve cystic fibrosis pediatric patients illustrate the use of this technology as a simple, painless, and reliable alternative to traditional hospital systems for measurements of sweat chloride.

1. Introduction

Cystic fibrosis (CF) is a common fatal genetic disease that demands continuous and careful management (Ruzal-Shapiro, 1998). Characterized by the production of thick, sticky mucus in the respiratory, digestive, and reproductive systems, CF can result in lung infections and

* Corresponding authorDivision of Pulmonary and Sleep Medicine, Ann & Robert H. Lurie Children's Hospital of Chicago, Chicago, IL, 60611, USA.
** Corresponding authorQuerrey Simpson Institute for Bioelectronics, Northwestern University, Evanston, IL, 60208, USA.
E-mail addresses: SMcColley@luriechildrens.org (S.A. McColley), jrogers@northwestern.edu (J.A. Rogers).
[1] These authors contributed equally: Joohee Kim, Seyong Oh, and Da Som Yang.

https://doi.org/10.1016/j.bios.2024.116166
Received 18 December 2023; Received in revised form 15 February 2024; Accepted 21 February 2024
Available online 23 February 2024

diminished lung function (Lyczak et al., 2002). Furthermore, digestive discomfort, such as poor nutrient absorption and gastrointestinal issues, further complicate the treatment of CF and afflict daily lives (Ooi and Durie, 2016). Evaluation of the concentration of chloride ions in sweat is the principal diagnostic test for CF, as commonly used in newborn screening (Beauchamp and Lands, 2005). Detection of elevated values of chloride performed via sweat collected from a patient and then transferred into a chloridometer for analysis represents the clinical standard. This test also can be used to monitor the progression of the CF condition and to guide timely adjustments to treatment regimens.

Although sweating can be induced by physical exercise or by exposure to hot, humid environments (ex, a warm water shower or bath) (Gao et al., 2016; Zhang et al., 2019), these options are generally not suitable for infants or most pediatric patients. An attractive and commonly used alternative relies on iontophoresis as a safe, simple, and painless process to deliver drugs that stimulate the action of eccrine glands through the surface of the skin non-invasively (Bariya et al., 2018; Lee et al., 2023; Sempionatto et al., 2021; Tu et al., 2023; Wang et al., 2022). Clinical standard systems rely on rigid, bulky hardware strapped tightly to the surface of the skin to capture sweat into coiled tubes following induction with separate pairs of electrodes and power supplies ("CF Sweat Testing," n.d.). The cost and complexity of this approach and the associated need for trained operators to perform the required procedures limits the use to specialized hospital facilities. This testing hardware also only applies to the measurement of chloride, without options in evaluating other biomarkers of potential relevance to the status of CF patients.

Recent research establishes the technology foundations for classes of devices that can mount gently on the surface of the skin for collecting sweat and performing in situ analysis of its chemical content, principally as the basis for physiological monitoring (Kim et al., 2019; Koh et al., 2016; Reeder et al., 2019). The simplest systems exploit soft, skin-compatible microfluidic systems with colorimetric assays for passive capture, storage and analysis of sweat rate, sweat loss and biomarker concentrations in sweat. Such devices are now in widespread commercial use for quantitatively measuring the loss of electrolytes and water through the natural release of sweat (Baker et al., 2020; "Gx Sweat Patch," n.d.). The process involves collection and analysis of digital images of the channel and reservoir structures of the device while on the skin, with established primary applications in sports performance and worker safety. An attractive feature of this technology is in its ability to be manufactured at scale, in cost effective continuous roll-to-roll processes, with options that support single-use modes of operation. Previous work demonstrates the applicability of this technology in testing for CF with pediatric patients, but with a requirement for separate means to stimulate the release of sweat (Ray et al., 2021). Unlike previous studies that focus solely on colorimetric detection methods or utilize conventional sweat collection techniques, our approach combines a compact iontophoresis system with a microfluidic structure, enabling analysis of chloride levels and other species in sweat after triggered activation of sweat glands. An alternative skin-interfaced platform for this purpose relies on integrated electronic components, batteries and radio hardware to induce sweat, to electrochemically evaluate its content and to wirelessly transmit the results to a separate device. (Choi et al., 2018; Emaminejad et al., 2017, 2017, 2017; Kim et al., 2016; Min et al., 2023; Tu et al., 2023; Wang et al., 2022). The large size, complexity, and cost of these research platforms create challenges in their commercial or clinical translation for widespread, routine use.

Here, we report a skin-interfaced, miniaturized wearable platform that combines the key advantages of these two distinct approaches, with demonstrations relevant to testing for CF and for care of patients with this condition but with a much wider range of potential applications. The device combines a simple electronic circuit, a manual switch, electrodes, hydrogels that include pilocarpine, colorimetric biosensors, microfluidic channels and microreservoirs, all within in a soft, flexible encapsulating structure. This miniaturized platform requires only microliters volume of sweat, thereby allowing rapid quantitative monitoring of various biomarkers from small regions of the skin. This feature represents a significant advance over standard clinical methods, which often require comparatively large volumes of sweat and complex procedures. Additionally, our device offers enhanced portability and convenience, as it is compact and wearable without imposing significant burden on the user. In demonstrations reported here, the platform includes separate microreservoirs and assays not only for chloride, an essential indicator for CF, but also for zinc and iron as species to monitor nutritional deficiencies that many CF patients experience due to digestive problems and malabsorption. Feasibility studies include monitoring of these species in five human subjects before and after a meal, with comparisons to standard laboratory analysis results. Additional work includes screening for five pediatric patients with CF, to compare the simplicity in operation, the reliability in evaluation and the accuracy in quantitative measurements of chloride to clinical standard systems used for this purpose in hospital settings.

2. Methods

2.1. Fabrication of the circuit, hydrogel, and microfluidic device

An ISO 9001-compliant PCB (printed circuit board) manufacturer provided the fPCB (flexible printed circuit board) based on designs created using Eagle CAD (Autodesk). A coating of gold (200 nm) deposited by electron beam evaporation on the anode and cathode prevented copper oxidation and corrosion. An In/Ag soldering paste (Indium Corporation) bonded the electronic components (coin-cell battery, tactile switch, low-dropout voltage regulator, DC/DC converter, red LED, capacitors, and resistors) to the fPCB. Use of a heat gun during the application process ensured fast and strong bonding.

A 4% agarose gel was prepared in a glass bottle by melting the agarose in deionized water, and pH buffer using a microwave and then cooling to 50 °C on a hot plate. Pilocarpine drug was then added to the gel to form a 0.5% concentration of pilocarpine hydrogel. The gels resulted from pouring the resulting liquid into a silicone mold with a depth of 3 mm at room temperature. The hydrogel was immediately transferred into a sealed container and wrapped with parafilm to minimize moisture loss. The pilocarpine concentration in the hydrogel was set to 0.5% to facilitate comparison with clinical standards. The clinical standard (Macroduct product) utilizes a pilocarpine concentration of 0.5%.

A thin layer of photoresist (KMPR 1010; MicroChem, MA, USA) spin-cast (3000 rpm for 30 s) on a silicon wafer (1 mm thick) and then patterned by photolithographically defined the geometry of the microfluidic system, including the microchannels, the microreservoirs, and the passive valves. After patterning, deep reactive ion etching (STS Pegasus ICP-DRIE, SPTS Technologies Ltd.) created trenches with depths of 200 μm. During the etching process, a thin layer of a fluorinated polymer (CFn) formed on the surface facilitated release from the mold. After fabrication of this mold, a mixture of a white dye (Reynolds Advanced Material, IL, USA, 10 wt%) and a precursor of PDMS (10:1 ratio of base to curing agent; Sylgard 184, Dow Corning, MI, USA) was spin-cast on the mold at 200 rpm for 30 s and baked at 70 °C for 2 h. After curing, the microfluidic layer was peeled from the mold. A mechanical biopsy punch defined 0.3 mm diameter inlet holes. Drop casting delivered assays for each biomarker into the microreservoirs. Separately, a uniform layer of PDMS (10:1) spin-cast (400 rpm for 30 s) and cured (70 °C for 2 h) served as a 100 μm thick cover layer bonded to the molded base using a corona treatment process. A mechanical die cutter defined the outer perimeter of the microfluidic system and two openings for the hydrogels.

2.2. Encapsulation of the circuit, and microfluidic device

A pair of convex (with holes) and concave (with pillars) aluminum

molds for the top encapsulation layer of the device was designed using SOLIDWORKS 2019 (Dassault Systemes) and formed using a milling machine (MDX-540, Rolland DGA). A silicone layer (PDMS, mixed with 5 wt% white silicone dye) cast against these molds and thermally cured at 100 °C for 20 min defined the top encapsulation layer. Integration of the electronic circuit within the top encapsulation layer was achieved using a silicone polymer (Ecoflex 0035, fast cure material). Curing and solidification occurred within approximately 10 min, thereby eliminating the need for a thermal curing step, and securely attaching the circuit to the upper encapsulation. Application of a medical-grade adhesive film (1524 skin adhesive, 3M) on both the top encapsulation containing the integrated circuit and the bottom microfluidic channel created a cohesive assembly.

2.3. Development of colorimetric assays for CF-biomarkers

Colorimetric chemical reagents, described in the following text, were drop cast into each microreservoir and dried in a desiccator.

(1) Chloride: 50 mg of silver chloranilate (MP Biomedicals, CA, USA) dispersed in 200 μL of 2 wt% polyhydroxyethylmethacrylate (Sigma-Aldrich, MO, USA) methanolic suspension. A volume of 0.5 μL of this solution was cast and dried in a corresponding reservoir.
(2) Zinc: The materials were purchased from Abcam (Cambridge, UK). The solution was prepared by mixing a 5-Br-PAPs solution and a solution of salicylaldoxime at a ratio of 4:1 volume. A volume of 1 μL of this solution was cast and dried in a corresponding reservoir.
(3) Iron: The material was purchased from Abcam (Cambridge, UK). A volume of 1 μL of Ferene-S solution was cast and dried in a corresponding reservoir.

2.4. Imaging sweat glands and characterizing their densities

Bromophenol blue was dissolved in pure acetone in a 5% (w/v) solution and then mixed with silicone in 1:1 volumetric ratio. The mixture was magnetically stirred at 25 °C until the acetone evaporated away and an orange solution was formed. The skin surface was washed and dried before spreading the bromophenol dye in a thin layer. Reaction with sweat from activated glands turned the orange dye blue in those regions within a few minutes.

2.5. Characterization and analysis

The temperature was measured using an IR camera (FLIR Systems, Wilsonville, OR, USA) and analyzed using the FLIR ResearchIR software (Research IR Max, FLIR Systems). The transmittance of the samples was measured by ultraviolet–visible–near infrared spectroscopy (PerkinElmer LAMBDA 1050, MA, USA). For this characterization, a transparent microfluidic channel was used instead of a white microfluidic channel. Average values and error bars were calculated using Excel (Microsoft). Each data point indicated the average of measurements, and the error bars represented the standard deviations (SDs). Pearson correlation with two-tailed p values analysis was conducted using the SPSS statistical software (IBM, NY, USA) and Origin Pro 9.0 software (Origin Lab, MA, USA).

The commercial software Ansys Maxwell was used to study the electric field generated by electrodes with square and circular shapes inside the skin. The relative permittivity (ε_r) and bulk conductivity (σ) were 1×10^6 and 0.1 $S{\cdot}m^{-1}$ for the skin. A current of 0.25 mA was applied to the electrodes. An adaptive mesh (tetrahedron elements) was adopted to ensure computational accuracy.

2.6. Sweat stimulation and color analysis with a ColorChecker

A test consisted of sweat stimulation (pilocarpine iontophoresis for 5 min) followed by sweat collection (~30 min), using either the Macroduct system or the skin-interfaced device reported here. In terms of Macroduct product, the test followed the instructions in the product catalog. Sweat was extracted from the collector after 30 min and analyzed using a chlorodimeter. For the skin-interfaced device, a digital image was recorded after removal from the arm, for quantitative analysis by color extraction algorithms. A digital image of the microfluidic device was captured along with an X-rite color checker, which served as a color reference. Regions of interest (ROIs) were carefully selected in the sensing reservoirs to avoid any defects. For image calibration, the color calibration transformation matrix was computed from the color values of the reference (Ray et al., 2021). The color values from the sensing reservoirs were converted to calibrated color values with the transformation matrix. The representative color parameters were carefully selected from the primary test; lightness (L*) in CIELab color space was used for chloride ion, whereas RGB values were used for zinc and iron level quantification. The final color intensities were converted to ion concentrations by using prior calibration curves determined from standard solutions..

2.7. Measurements of CF-related biomarker levels healthy human subjects' studies

Testing involved five healthy adults (aged 20–35) as volunteers. All subjects provided their consent prior to participation. Prior to sweat stimulation and monitoring, the skin was cleaned with an alcohol gauze pad and clean tissue with deionized water, followed by attachment of the skin-interfaced, miniaturized wearable systems on the forearms. Sweat collected by the Macroduct collector was analyzed using a lab-based instrument. The collected sweat samples were diluted into 3 mL 3% HNO_3, without the need for additional heating because of the absence of organic chelates to form with the metals. Diluted samples were analyzed by ICP-MS (Thermo iCap7600, Thermo Fisher Scientific, MA, USA). Colorimetric analysis from the skin-interfaced device yielded biomarker concentrations.

2.8. Clinical study design

The purpose of the clinical study was to demonstrate a skin-interfaced, miniaturized device for use in collecting and analyzing sweat for the diagnosis of CF. Patients were recruited from CF populations. The study was Institutional Review Board (IRB)–approved through the Ann & Robert H. Lurie Children's Hospital (IRB, 2018–1440). Patients with CF were recruited from the Cystic Fibrosis Center at Lurie Children's Hospital. Informed consent was obtained after the study was explained. The sweat tests were performed by trained personnel at Northwestern University and Lurie Children's Hospital. Patient sweat tests followed established clinical protocols. The pilot study ($N = 7$) was conducted to evaluate the performance of a developed device with an integrated colorimetric chloride assay. For the Macroduct system, chloride measurements were performed using a clinically certified ChloroCheck Chloridometer (ELITech Group).

3. Results

3.1. Design of the skin-interfaced, miniaturized wearable platform for evaluation of sweat biomarkers related to cystic fibrosis and nutritional balance

As shown in the schematic illustration of Fig. 1A, the device supports combined capabilities in stimulation, collection, and multicomponent biochemical analysis of microliter volumes of sweat. The elements include a disposable soft, microfluidic system with reagents that enable

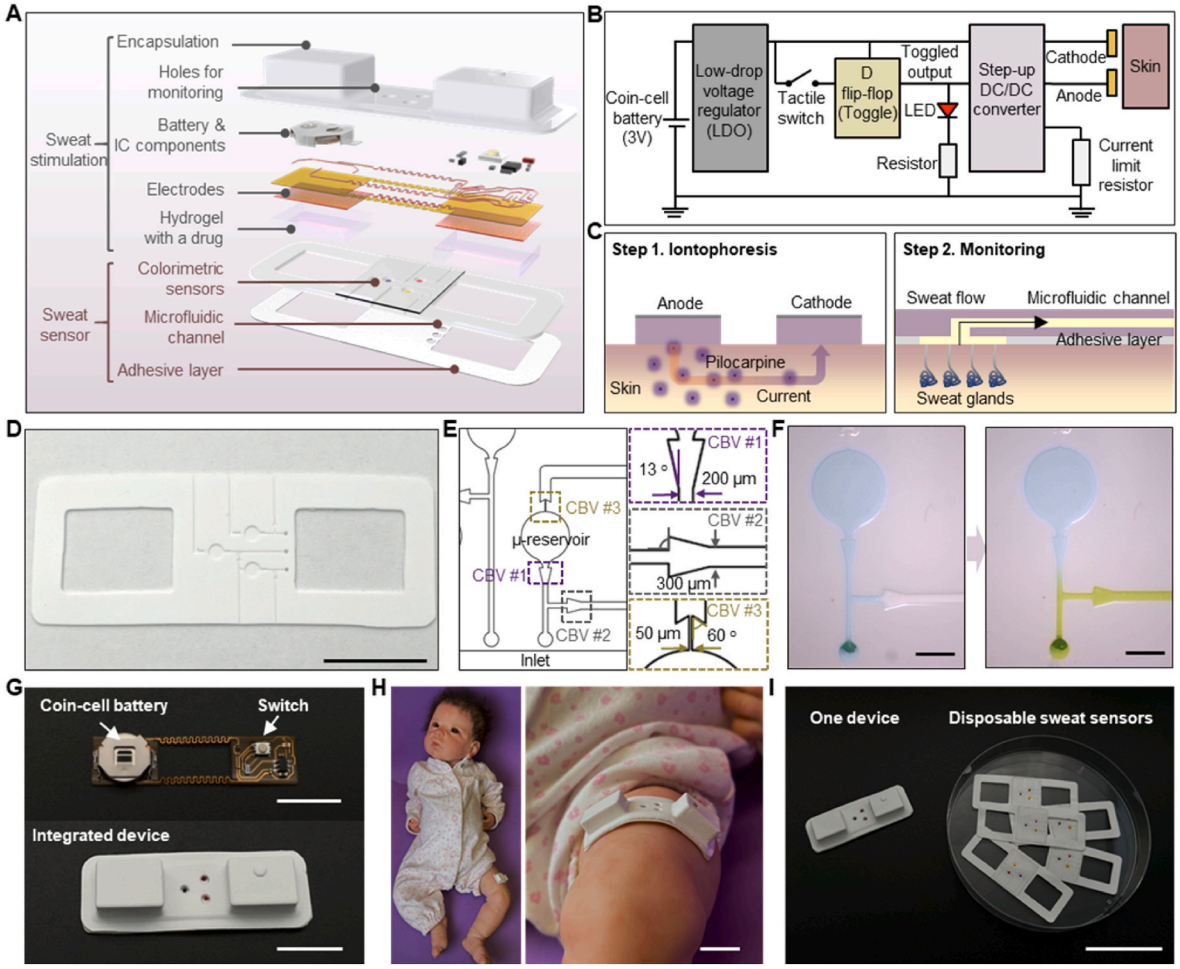

Fig. 1. Schematic illustrations and images of a skin-interfaced, miniaturized wearable platform for triggered induction, capture and colorimetric analysis of microliter volumes of sweat. (A) Schematic exploded view illustration of the design of system. (B) Block diagram of the operational scheme of the sweat triggering circuit with electrodes, a tactile switch, LED, and coin-cell battery. (C) Schematic illustrations of the iontophoresis step and sweat monitoring step. (D) Optical image of the microfluidic channel structure with CBVs. Scale bar, 1 cm. (E) Detailed schematic illustration of sampling inlet, microreservoir, and CBVs with different channel widths and diverging angles. (F) Optical images of the operation of the CBVs in guiding sweat into the microreservoir, and microfluidic channel. A dye was incorporated to enhance visualization, leading to a transition from light blue to yellow green. Scale bars, 1 mm. (G) Image of the sweat stimulation circuit (top), a fully integrated device with a circuit, and microfluidic sensor (bottom). (H) Images of a device on the thigh of a realistic model of a neonate. Scale bar, 2 cm. (I) Image of the completed device with several disposable sweat sensors. Scale bar, 2 cm.

colorimetric sensing of multiple biomarkers, a hydrogel with a cholinergic drug that stimulates eccrine sweat glands (pilocarpine), and a reusable, flexible electronics module that initiates delivery of this drug through the skin by iontophoresis. In the examples reported here, the sensing functionality enables precise measurements of the concentrations of chloride, zinc, and iron in sweat, the first of which is directly related to CF; the others provide insights into related aspects of nutritional status, all with sensitivity across physiologically relevant ranges for sweat. The system-level block diagram in Fig. 1B and the circuit layout in Fig. S1 illustrate the operation and circuit design, respectively. A flexible printed circuit board (fPCB, PCBWay; thickness: ~100 μm) supports a collection of surface-mount electronic components interconnected by copper traces in serpentine geometries to enhance the mechanical compliance. A small coin-cell battery (CR1025, Renata; diameter: 10 mm; thickness: 2 mm; 3 V; 30 mA h) and a low-dropout voltage regulator (TPS7A0318DBVR, Texas Instruments) provide a stable supply voltage of 1.8 V. Pressing a tactile switch generates a clock signal and toggles the electronic status of the D flip-flop (SN74AUP1G74YZPR, Texas Instruments) from Low to High or from High to Low, to activate or deactivate a step-up DC/DC converter (R1218, Ricoh Electronic Devices) that boosts the voltage from the battery to a range of 16–18 V sufficient to support the iontophoresis delivery process. A red LED indicates the operational status (Fig. S1B). As a safety mechanism, a limiting resistor ensures that the current remains below 0.25 mA, corresponding to a current density (2.5 μA/mm^2) that lies within a safe range for human skin. Gold serves as an inert electrode material to enable multiple cycles of use with little degradation.

Fig. 1C shows processes for sweat induction that follow from use of this system. The applied voltage causes positively charged pilocarpine molecules to move from the anode side of the system into the skin and toward the cathode, thereby activating sweat glands directly underneath and adjacent to the location of the hydrogel at the anode. Sweat induced at the adjacent regions enters into three inlets defined on the base of the soft (1–2 MPa; silicone elastomer) microfluidic system. This sweat passes through separate microchannels and passive microvalves (capillary bursting valves, CBVs) to three corresponding microreservoirs (Fig. 1D), each of which contains a different colorimetric reagent (for Cl, Zn, and Fe ions). When sweat flows through a single connected channel and encounters two separate CBVs with differing bursting pressures, it follows the path of least resistance by passing through the valve with the lower bursting pressure initially. This strategic placement of CBVs with varying pressures near channel intersections allows for precise control over the direction of flow. The measured bursting pressures of CBV #1, #2, and #3 are 0.4, 0.8, and 12 kPa, respectively (Fig. S2). Upon the

initial arrival of sweat at CBVs #1 and #2, CBV #1 opens to facilitate the flow into the microreservoir. Once the reservoir is adequately filled, the pressure of the sweat flow triggers the opening of CBV #2, which has a lower bursting pressure compared to CBV #3, ensuring a sequential flow of sweat through the microfluidic system. By this process, the microvalves prevent excess sweat from washing out the reagents in these microreservoirs by routing this sweat through connecting microfluidic channels and outlet ports (Fig. 1E and F). The microreservoirs have circular shapes with diameters of 2 mm and depths of ~200 μm, corresponding to volumes of 2~3 μL. This microfluidic system adopts the form of a thin (0.7 mm), rectangular shape (50 mm by 15 mm) with openings at the two ends for the hydrogels. The device, with all components co-integrated into a soft silicone encapsulating structure, appears in Fig. 1G. The small size (50 mm by 15 mm) and the flexibility of the system facilitates attachment onto various body locations for both infants and adults (Fig. 1H, and Fig. S3) using a mild, medical grade adhesive (1524 skin adhesive, 3M, Inc.; thickness 60 μm). Openings in this adhesive define areas for collecting sweat and delivering the pilocarpine, with a water-tight seal to the surrounding areas of the skin for efficient sweat collection without leakage or contamination from the hydrogel (Fig. S4). The system can be used many times (~19 times) with a single coin-cell battery, in a mode where the microfluidic component is a single-use disposable (Fig. 1I, and Fig. S5). Additional details of the fabrication and integration strategies are in Fig. S6 and the Methods.

By comparison, the clinical product for sweat collection and analysis (Macroduct® Sweat Collection System, ELITechGroup) involves three separate parts (Fig. S7): one that delivers pilocarpine; another that collects induced sweat (plastic housing, elastic strap and coiled tube); and a third that analyzes the concentration of chloride in the sweat. The first part activates the sweat glands by use of an external power supply (width: 18 cm, depth: 14 cm, height: 5 cm), a set of wired electrodes (electrode size: 6 cm^2, wire length: 15 cm) that connect to the supply, pilogel discs (disc size: 6 cm^2, thickness: 6 mm) that load onto the electrode surfaces, and a strap (width: 2 cm and length: 25 cm) that presses the system onto the skin. The second part collects the induced sweat into a coiled tube (diameter: 2 mm, length: 30 cm) contained in a rigid housing (oval size: 6 cm^2), also with a strap to ensure a tight seal to the skin. Collection of at least 15 μL of sweat, 7 times more than that required for the platform reported here, enables analysis by a benchtop external instrument (25 cm x 30 cm x 20 cm) (Fig. S7), as the third part of the system for analysis of the chloride concentration in sweat extracted from the tube. The large, cumbersome nature and cost of this three-part system, the difficulty in collecting sufficient sweat for analysis, and the potential for contamination during transfer of sweat from the tube to the analysis instrument, confines its use to trained personnel in hospital or laboratory environments.

3.2. Design, characterization, and safety of the iontophoresis system

The parameters for iontophoretic delivery of pilocarpine and the responses of the activated sweat glands are important design considerations. The square shape of the electrode leads to release of sweat uniformly across each inlet of the sweat microfluidic structure, as illustrated in Fig. 2A. Simulation results indicate that the maximum electric field in the skin is ~300 V/m for this geometry (Fig. 2B, and Fig. S8), which was about 16 times smaller than the regulatory limit (5000 V/m) ("Radiation," n.d.), and that the electric field extends to areas adjacent to the electrode. Application of bromophenol dye to the skin allows visualization of sweat glands activated by this iontophoresis process, as described in the Methods section (Tashiro et al., 1961). Studies on three subjects (two females and one male) with iontophoresis applied for 5 min on the forearm (Fig. 2C) reveal average densities of activated sweat glands of 28 and 23 glands/0.25 cm^2 for regions within the areas of the anode and immediately adjacent to it on the side facing the cathode, respectively (Fig. 2C and 2D). This adjacent region is, therefore, a valuable location for capturing sweat through inlets to the microfluidic structure. In iontophoretic delivery, the pilocarpine hydrogel also plays a crucial role. Immediate transfer to containers and wrapping in parafilm after forming the hydrogels minimizes evaporative losses. Experimental assessments of evaporation during storage appear in Fig. S9.

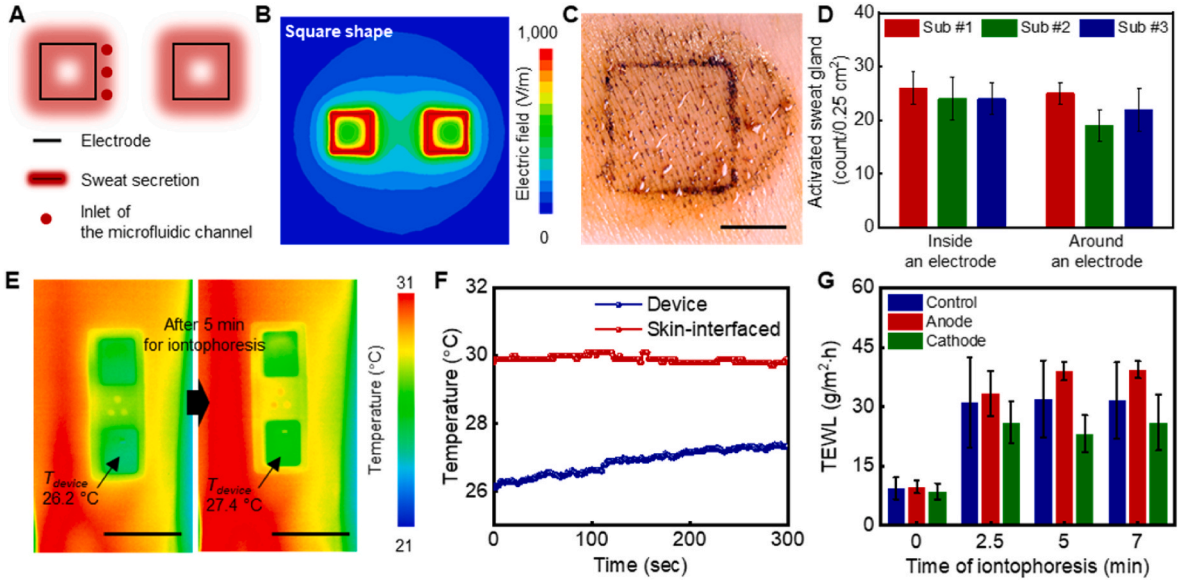

Fig. 2. Design, characterization, and safety profile of the iontophoresis system. (A) Illustration of the inlet location of the microfluidic channels relative to the rectangular electrodes. (B) Electric field distributions on the surface of the skin for electrodes with square shapes during iontophoresis operation. (C) Photograph of sweat glands imaged with bromophenol blue on the forearm after 5 min iontophoresis. The dark square indicates the location of the anode. Scale bar, 1 cm. (D) Sweat gland densities at the location of the anode and adjacent to it (one representative image: Fig. 2C) for three subjects. Each data point represents the mean ± SD. (E) Infrared image of an operating device applied on the skin of healthy subject for evaluating the effects of heat generated by the iontophoresis process. Scale bar, 1 cm. (F) The temperature of the device and the skin interfaced with the device during the device operation for 5 min. (G) TEWL measured prior to iontophoresis (plotted at time = 0) and 7 min following either 2.5, 5, and 7 min of current passage at 0.25 mA. Results for the skin sites below the anode and cathode after operation for various times, and a control case that does not involve operation. Each data point represents the mean ± standard deviation for five subjects.

Monitoring the mass of the hydrogel over seven days reveal no significant changes, indicating the effectiveness of the storage conditions in preventing evaporation.

Further studies focus on aspects related to safe operation of the device, including parasitic heating that can occur during iontophoresis (Moritz and Henriques, 1947) and associated alterations in the trans-epidermal water loss (TEWL) or skin pH. For the first, an infrared camera and thermocouple provide precise measurements of heating during operation of the device for 5 min (Fig. 2E and 2F). Results with a healthy human subject (Female, 30 years old) indicate that the temperature of the skin remains relatively unchanged, at ~30.1 °C, while the temperature of the surface of the device increases slightly from 26.2 °C to 27.4 °C. Evaluations of TEWL using a commercial meter (gpskin barrier pro, GPower Inc., Korea; a contactless measurement using humidity and temperature sensors) provide insights into possible irritation to the skin and/or disruptions in barrier function (Honari and Maibach, 2014). The sites of measurement before and after use of the device include those at the location of the anode and the cathode and at a nearby region away from the device but exposed to the same hydrogel (Fig. S10A), across healthy subjects. The results for cases of iontophoresis (without pilocarpine) at 0.25 mA for 2.5, 5 and 7 min appear in Fig. 2G. TEWL increases with the time of application (anode: from 9.8 ± 1.6 g/m^2·h to 39.0 ± 2.3 g/m^2·h, cathode: from 8.6 ± 2.0 g/m^2·h to 23.2 ± 4.6 g/m^2·h, and control: from 9.4 ± 2.7 g/m^2·h to 32.0 ± 9.7 g/m^2·h after 5 min iontophoresis). The site exposed to the hydrogel for the same period of time but without iontophoresis shows similar results. The changes in TEWL can, therefore, be associated with the hydrating effects of the hydrogel, unaltered by the iontophoresis process. Additional information follows from assessments of skin pH using a commercial meter (Skin pH tester, Hanna Instruments, USA) applied to five healthy subjects before and after the iontophoresis process. These measurements examine the possibility that iontophoresis leads to some electrolysis of water, with potential for associated changes in pH by generation of H^+ and OH^- at the anode and cathode, respectively. As shown in Fig. S10B, the changes in skin pH are small (anode: from 5.2 ± 0.4 to 5.1 ± 0.4, and cathode: from 5.2 ± 0.5 to 5.1 ± 0.4), with values that lie within a normal range for skin (4.7–5.7) (Lambers et al., 2006).

3.3. Quantitative colorimetric analysis for monitoring of biomarkers related to CF and nutritional balance

As discussed previously, a high concentration of chloride in sweat is a well-established marker for CF. The other species analyzed here relate to nutritional status, with specific additional relevance to patients with CF. For example, zinc and iron deficiency can follow from poor protein digestion and fat malabsorption (Dodge and Turck, 2006; Engelen et al.,

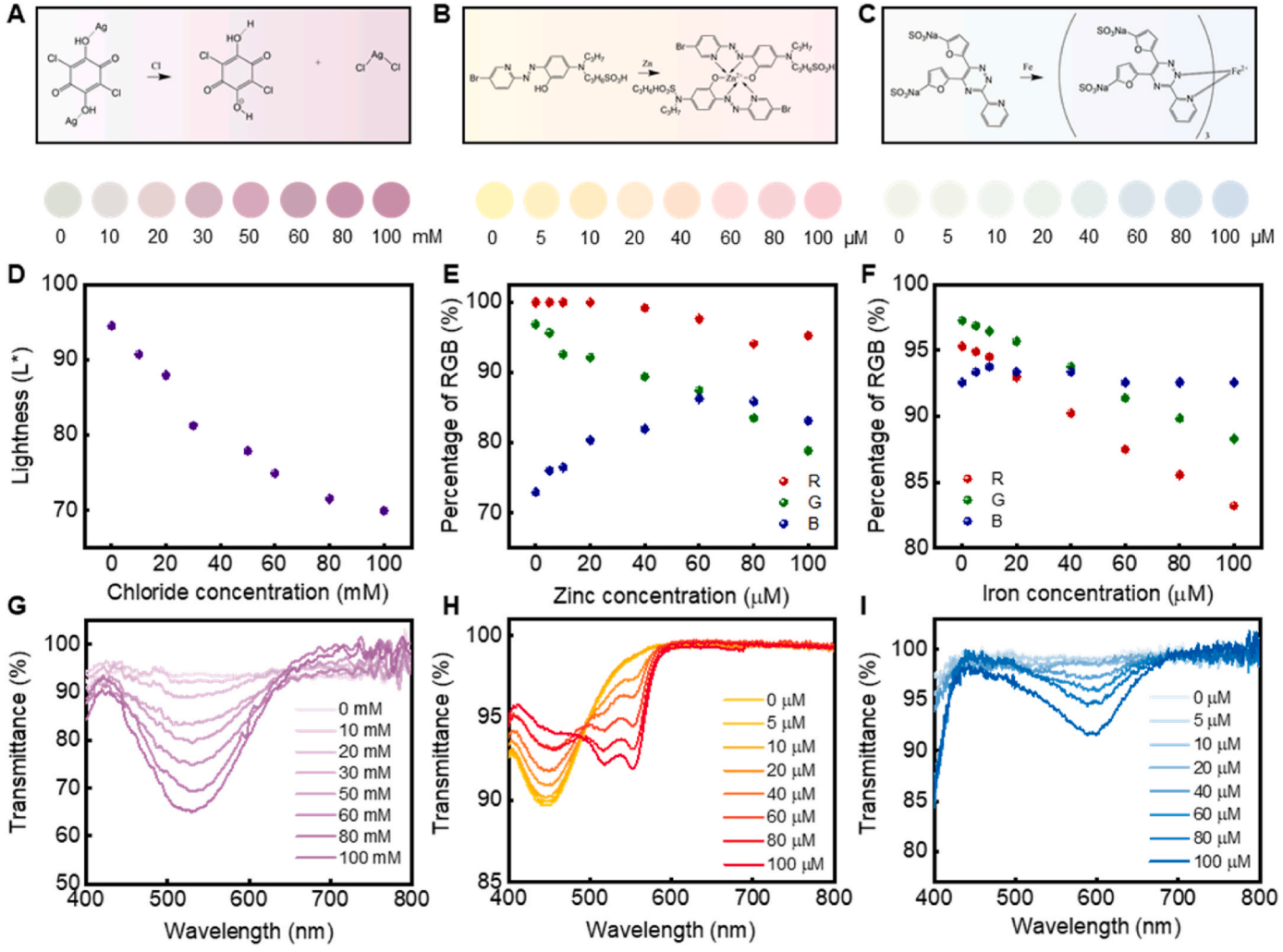

Fig. 3. Quantitative colorimetric analysis of the concentrations of chloride, zinc and iron assays by optical image processing and ultraviolet (UV)-visible spectroscopy. Color response of the assays through 200 μm-thick microfluidic channels at various concentration of (A) chloride (B) zinc, and (C) iron. Standard calibration curve at various concentrations of (D) chloride (E) zinc, and (F) iron. Each point indicates the average value of three samples, and the error bars represent the standard deviation. The measured spectral transmittance at various concentration of (G) chloride, (H) zinc, and (I) iron.

2014; Escobedo Monge et al., 2019). Deficiency of these minerals can lead to a broad range of consequences and symptoms, such as stunted growth, delayed sexual maturation, disturbed immunity, and anemia, each of which is frequently present in patients with CF (Van Biervliet et al., 2007). In particular, young infants, because of their rapid growth rate, have relatively high physiologic requirements for zinc and iron (Krebs et al., 2000). Approximately 35% of children with CF are either nutritionally 'at risk' or in 'urgent need' of nutritional intervention and rehabilitation (Escobedo Monge et al., 2019). For these reasons, monitoring of nutrition is important, therefore motivating our development of a single platform capable of measuring zinc, iron and chloride concentrations in sweat by colorimetric reagents integrated into the microfluidic system. This scheme affords an ability to measure these concentrations in situ during and immediately after sweat collection, without need for integrated electrochemical sensors or for sweat extraction and measurement with external instruments. Silver chloranilate suspended in polyhydroxyethyl methacrylate solution serves as the colorimetric sensor for chloride, following a reaction that produces a purple color, as described previously (Ray et al., 2021) (Fig. 3A). A drop-casting procedure loads this reagent into the microreservoirs. Similar casting schemes yield assays for zinc, and iron. The zinc sensor uses 2-(5-Bromo-2-pyridylazo)-5-[N-propyl-N-(3-sulfopropyl)-amino]-phenol (5-Br-PAPs) as a chelating agent that binds zinc with high affinity, leading to a color change from yellow to pink (Fig. 3B) (Wang et al., 2018). As shown in Fig. 3C, iron relies on 3-(2-pyridyl)-5,6-difurylsulfonic acid-1,2,4-triazine disodium salt (Ferene-S) to produce a blue complex (Hirayama and Nagasawa, 2017).

Fig. 3D–F shows the lightness ('L*' from black (0) to white (100)) for the chloride sensor and extracted RGB values for the zinc and iron sensors for various concentrations from digital images captured with a color balance reference (ColorChecker; Fig. S11A) using a digital single-lens reflex (dSLR) camera or smart phone camera under ambient lighting or, for highest accuracy, controlled lighting conditions (light box, Fig. S11B, luminance: 900 Lux). Additional details of the digital imaging-based quantification for each ion are in Fig. S12 and the Methods. Calibration curves reveal linear relationships between the lightness and the concentration of chloride (0.25 L*/mM, Fig. 3D) and between the green (G) value and the concentration of zinc and iron (0.15 %/μM, Fig. 3E; 0.1 %/μM, Fig. 3F). By the metric 3σ/slope (σ: the standard deviation, slope: the slop between the color response versus concentration), the detection limits of chloride, zinc, and iron are 0.8 mM, 0.7 μM and 1.2 μM, respectively. Established guidance is that chloride concentrations below 30 mM are normal, between 30 mM and 60 mM suggest some symptoms of CF, and greater 60 mM strongly indicate that the patient has CF (Farrell et al., 2008). As shown in the calibration curve (Fig. 3D), the sensor covers this full range of concentrations (0–100 mM). For zinc and iron, healthy individuals have concentrations of 5–17 μM and 0.4–20 μM, respectively (Kim et al., 2022). As with chloride, the colorimetric sensors for zinc and iron also cover the physiologically relevant ranges. Measurements by ultraviolet (UV)-visible spectroscopy (Fig. 3G–I) yield results similar to those obtained from digital images.

Additional experiments define the dependence of the chloride assay on pH, temperature, and time. Sweat is normally slightly acidic, with pH typically between 4.5 and 7.0. Results of tests in buffer solutions with pH 4, 5, 6, and 7, as shown in Fig. S13A, indicate that the responses of the chloride assays change the sensitivity by only 0.001 L*/mM over this range. The temperature of the sweat, enclosed in devices that are in intimate contact with the skin, is comparable to that of the body, between 33.5 and 36.9 °C. Results obtained from 20 °C to 40 °C reveal negligible dependence of the response on temperature, with a decrease in sensitivity of only 0.002 L*/mM (Fig. S13B). Stability studies of zinc and iron sensors reported previously (Kim et al., 2022), demonstrate similarly low levels of sensitivity to pH and temperature. Measurements of the time dependence of the colorimetric response of the chloride sensor reveal saturation within approximately 10 min (Fig. S13C). Previous reports on the zinc and iron sensors indicate similar behaviors (Kim et al., 2022). The chloride, zinc, and iron sensors measure the concentration of each biomarker in sweat that enters the microfluidic channel. Residual pilocarpine from the hydrogels has the potential to be present in the sweat that enters the device. Experiments to investigate the possible effects, as shown in Fig. S14, involve measurements of the color change of the chloride, zinc, and iron sensors in the presence and absence of pilocarpine. The results indicate that the effect of pilocarpine on the colorimetric assays is negligible.

3.4. On-body tests of healthy human subjects before and after a meal

Dietary adjustments and nutritional management are important aspects of the treatment and care of all individuals, but especially those with CF. Due to challenges in digesting and absorbing nutrients properly, patients with CF often require specialized dietary considerations. Studies reported here, therefore, examine changes in chloride, zinc and iron concentration before and after dietary intake. Tests with healthy human subjects involve controlled dietary intake (three males and two females) to demonstrate key features of the integrated device (mounted on the left forearm) with control measurements (on the right forearm) performed using a commercial system and analysis with laboratory instruments. Details are in the Methods section. One set of experiments shows that the concentration of each of the sweat biomarkers studied here increases after a meal (Fig. 4A–C) following overnight fasting, as determined using both systems. Specifically, before the meal, the concentrations are 1.6 mM–26.8 mM for chloride, 6.9 μM–15.1 μM for zinc, and 0.9 μM–2.5 μM for iron. After the meal, these values increase to 5.4 mM–27.0 mM for chloride, 9.3 μM to 22.1 μM for zinc, and 2.8 μM–7.3 μM for iron.

Comparisons between sweat samples analyzed ex situ by inductively coupled plasma-mass spectrometry (ICP-MS) and in situ by colorimetric evaluations (Fig. 4D–F) show Pearson correlation coefficients of 0.976, 0.988, and 0.891 with the low two-tailed p value ($^{**}p < 0.01$ for chloride, $^{**}p < 0.01$ for zinc, and $^{**}p < 0.01$ for iron) for concentrations of chloride, zinc, and iron sensing, respectively.

3.5. Clinical studies of patients with cystic fibrosis

Studies to demonstrate clinical utility involve patients with CF evaluated at the Cystic Fibrosis Center at the Ann & Robert H. Lurie Children's Hospital (Chicago, IL). Bilateral testing enables comparisons between the device reported here and the clinically established standard described previously (Macroduct). Fig. 5A shows a representative pediatric participant wearing both devices during a clinical evaluation. The clinical standard with wired electrodes and tight straps is on the right arm. A gentle adhesive holds the device introduced here to the left arm. Photographs of other participants wearing both devices are in Fig. S15. Table S1 summarizes the participant demographics and ages ($N = 7$). Fig. 5B highlights the components utilized in both systems, to emphasize the simplicity and ease of use of the technology introduced here. Fig. 5C and D depict the testing processes. For the clinical standard product, the first step involves fastening wired electrodes to the arm using a strap (Fig. 5D, step 1). A technician then initiates sweat stimulation via a control system (Fig. 5D, step 2), and upon completion, removes the electrodes (Fig. 5D, step 3). Next, the rigid, plastic housing sweat collector is carefully aligned and affixed to the stimulated area using another strap to apply sufficient pressure to form an adequate seal (Fig. 5D, step 4). After 30 min for sweat collection, the technician removes the protective transparent cover from the sweat collector and then carefully inserts the syringe into the tube. The tube is uncoiled from the collector and severed using a nipper. Immediately after severing the tube, the technician uses the plunger to draw the sweat from the tube. (Fig. 5D, steps 5–7) and loads it into dedicated equipment for analysis (Fig. 5D, step 8). In contrast, the device reported here offers a much more streamlined approach. After attaching to the skin (Fig. 5C, step 1) and activating via the switch (Fig. 5C, step 2), sweat begins to collect into the microfluidic channels and microreservoirs. Following the

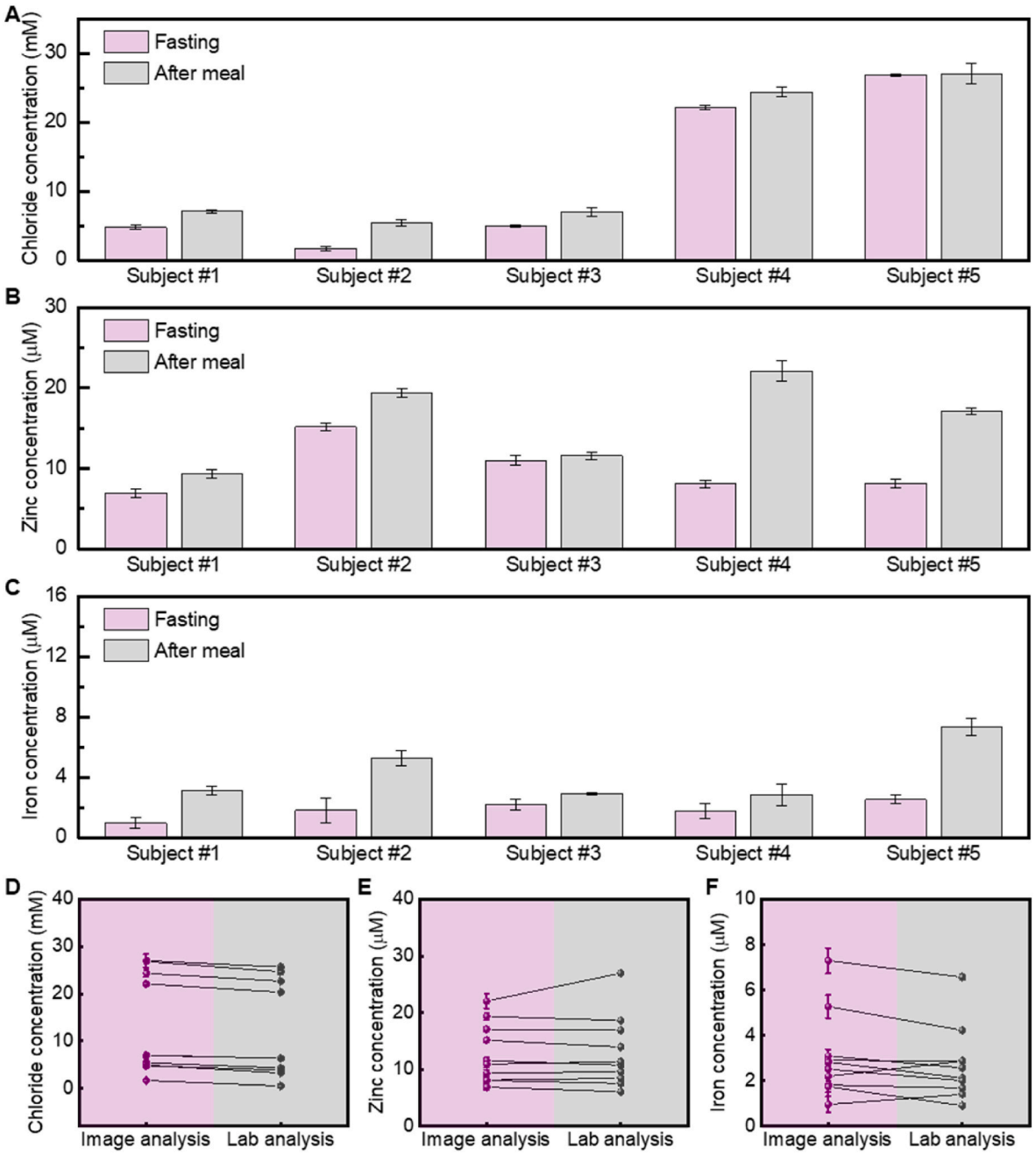

Fig. 4. Human trials for the system and comparisons to lab analysis, before and after taking a meal. Measured sweat concentrations of (A) chloride, (B) zinc, and (C) iron by colorimetric image analysis before and after taking a meal. The error bars represent the standard deviations. Validation of the colorimetric approach for analyzing (D) chloride, (E) zinc, and (F) iron in sweat samples through comparisons to results obtained by lab analysis. The data are based on sweat samples collected from healthy human subjects (n = 5).

clinical standard protocol (Macroduct product), sweat collection proceeds for 30 min to ensure sufficient quantities of sweat for analysis. By contrast, due to the small volumes (2–3 μL) of the microfluidic reservoirs, filling can occur in less than 30 min. Furthermore, the microvalves in our microfluidic system direct excess sweat to outlet ports. This design feature ensures that measurements can be performed at any time after the reservoir fills. The device can then be removed after sweat collection (Fig. 5C, step 3), for immediate colorimetric without further manipulation or transfer, or access to additional equipment other than a camera (Fig. 5C, step 4). During step 3, careful handling eliminates the possibility of expelling sweat from the device during removal (Fig. S16).

Among seven patients, one complained of pain during sweat stimulation and one did not yield sufficient sweat (~15 μL), both with the clinical standard product, thereby preventing collection and comparison in those two cases. Fig. 5E shows that results for the remaining five patients indicate excellent agreement between the two measurements, all within uncertainties (Correlation coefficient = 0.98) with the two-tailed p value ($^*p < 0.05$). Additional evaluations focus on the level of pain associated with these two methods, across a scale from 0 (no pain) to 10 (high pain). As shown in Fig. 5F, the average pain levels for the device reported here are ~2, a factor of two less than those of the clinical standard product. Fundamental design improvements evident in our device as compared to the Macroduct product include a method for device attachment, sweat visualization, and patient comfort.

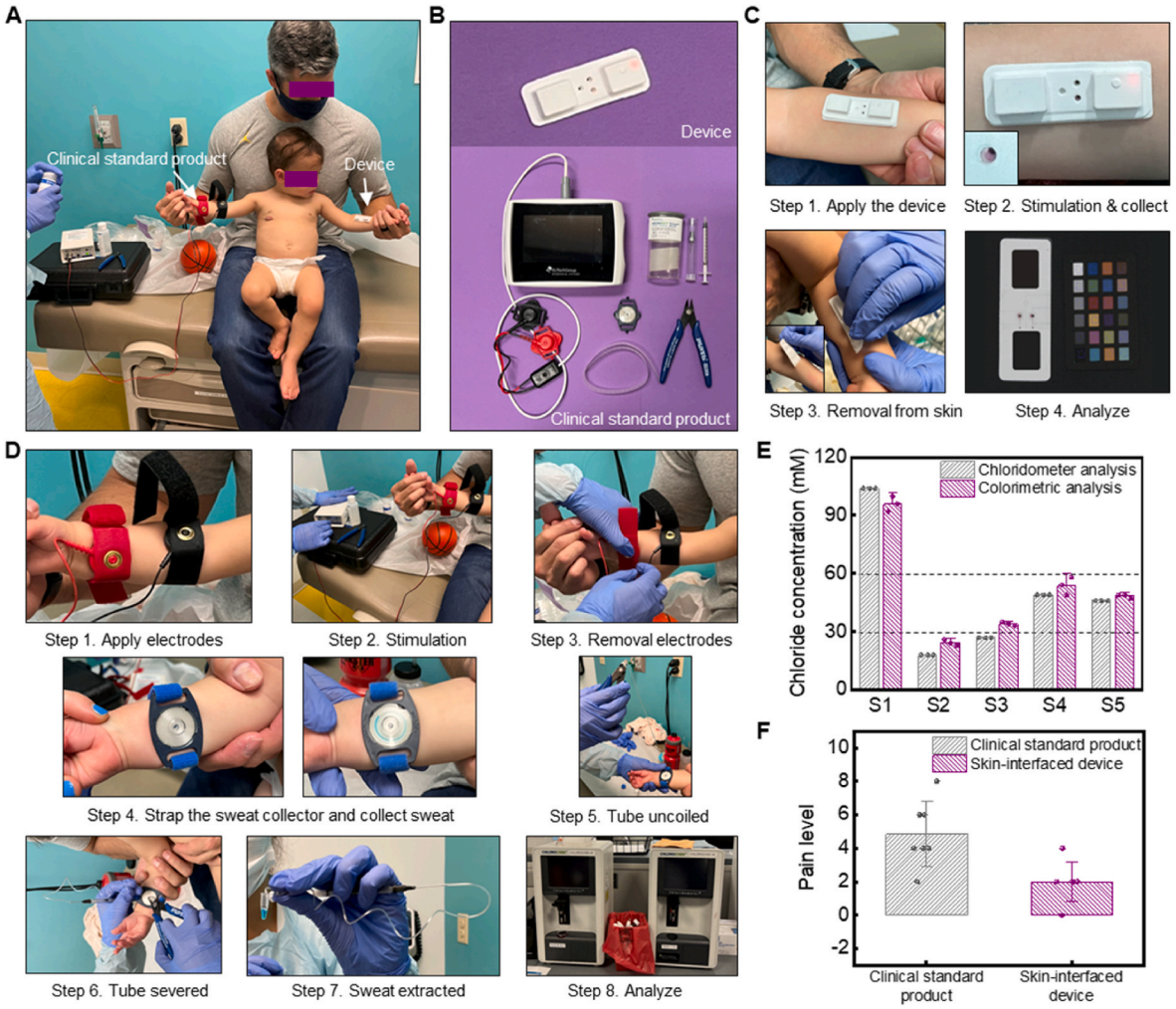

Fig. 5. Pictures and results from clinical studies of the system, with comparisons to the standard process. (A) Representative photograph of a pediatric subject undergoing a sweat test procedure. The clinical standard product is on the right arm, featuring wired electrodes secured with straps. The system introduced here is on the left arm. (B) Comparison of the components involved in the clinical standard test and the system introduced here. (C) Images of the four steps for conducting the test using the system introduced here. (D) Pictures of the eight steps for performing the test using the clinical standard product. (E) Comparison of chloride values in sweat between two methods (colorimetric analysis and chloridometer) in clinical studies of pediatric patients with cystic fibrosis (n = 5). (F) Pain levels experienced with these two systems, for seven patients. Each point indicates the pain level, and the error bars represent the standard deviation.

4. Discussion and conclusion

This report introduces a skin-interfaced, miniaturized soft microfluidic platform that can monitor the concentrations of chloride, zinc, and iron in sweat, as parameters relevant to screening for cystic fibrosis and tracking the health of patients with this disease. Colorimetric assays provide the basis for measurements of these biomarkers in microreservoirs filled with sweat stimulated by iontophoretic delivery of pilocarpine through the skin using a compact, simple electronic system. Demonstration studies that include both healthy participants and cystic fibrosis pediatric patients illustrate the ease-of-use of the technology as well as its reliability and accuracy in operation, benchmarked against laboratory instruments and clinical standard assays (Macroduct). A key advantage of the device is in its ability for use outside of hospital settings, without the need for trained personnel. The consequences allow applications in remote or resource-limited regions, with immediate implications in health equity. Future studies will examine the use of similar concepts for evaluating other sweat biomarkers of interest to additional classes of patients.

CRediT authorship contribution statement

Joohee Kim: Writing – review & editing, Writing – original draft, Visualization, Validation, Investigation, Conceptualization. **Seyong Oh:** Methodology. **Da Som Yang:** Validation. **Larissa Rugg:** Investigation. **Radhika Mathur:** Investigation. **Sung Soo Kwak:** Methodology. **Seonggwang Yoo:** Methodology. **Shupeng Li:** Software. **Evangelos E. Kanatzidis:** Data curation. **Geumbee Lee:** Validation. **Hong-Joon Yoon:** Validation. **Yonggang Huang:** Software. **Roozbeh Ghaffari:** Validation. **Susanna A. McColley:** Supervision. **John A. Rogers:** Writing – review & editing, Supervision.

Declaration of competing interest

Roozbeh Ghaffari and John A. Rogers are co-founders of a company, Epicore Biosystems, that develops and commercializes microfluidic devices for sweat analysis.

Acknowledgments

This work was supported by the Querrey-Simpson Institute for Bioelectronics at Northwestern University. This work made use of the

NUFAB facility of Northwestern University's NUANCE Center, which had received support from the SHyNE Resource (Grant No. NSF ECCS-2025633), the IIN, and the Northwestern's MRSEC program (Grant No. NSF DMR-1720139); the Keck Foundation. J.K. acknowledges additional support by KIST Institutional Program [Project No. 2E33141, and 2N70970], the Ministry of Science & ICT (MSIT) of Korea through National Research Foundation (Grant No. RS-2023-00211342), and grant of the Korea Health Technology R&D Project through the Korea Health Industry Development Institute (KHIDI), funded by the Ministry of Health & Welfare, Republic of Korea (Grant No. HI19C1348). We also acknowledge the clinic study support from the Ann &Robert H. Lurie Children's Hospital.

Appendix A. Supplementary data

Supplementary data to this article can be found online at https://doi.org/10.1016/j.bios.2024.116166.

References

Baker, L.B., Model, J.B., Barnes, K.A., Anderson, M.L., Lee, S.P., Lee, K.A., Brown, S.D., Reimel, A.J., Roberts, T.J., Nuccio, R.P., Bonsignore, J.L., Ungaro, C.T., Carter, J.M., Li, W., Seib, M.S., Reeder, J.T., Aranyosi, A.J., Rogers, J.A., Ghaffari, R., 2020. Skin-interfaced microfluidic system with personalized sweating rate and sweat chloride analytics for sports science applications. Sci. Adv. 6, eabe3929.

Bariya, M., Nyein, H.Y.Y., Javey, A., 2018. Wearable sweat sensors. Nature Electronics 1, 160–171.

Beauchamp, M., Lands, L.c., 2005. Sweat-testing: a review of current technical requirements. Pediatr. Pulmonol. 39, 507–511.

CF Sweat Testing [WWW Document], n.d. URL https://macroductadvanced.com/index.html (accessed 12.14.23).

Choi, D.-H., Thaxton, A., Jeong, I., Kim, K., Sosnay, P.R., Cutting, G.R., Searson, P.C., 2018. Sweat test for cystic fibrosis: wearable sweat sensor vs. standard laboratory test. J. Cyst. Fibros. 17, e35–e38.

Dodge, J.A., Turck, D., 2006. Cystic fibrosis: nutritional consequences and management. Best Practice & Research Clinical Gastroenterology, Nutritional and Dietary Consequences of Gastronintestinal Diseases 20, 531–546.

Emaminejad, S., Gao, W., Wu, E., Davies, Z.A., Yin Yin Nyein, H., Challa, S., Ryan, S.P., Fahad, H.M., Chen, K., Shahpar, Z., Talebi, S., Milla, C., Javey, A., Davis, R.W., 2017. Autonomous sweat extraction and analysis applied to cystic fibrosis and glucose monitoring using a fully integrated wearable platform. Proc. Natl. Acad. Sci. USA 114, 4625–4630.

Engelen, M.P.K.J., Com, G., Deutz, N.E.P., 2014. Protein is an important but undervalued macronutrient in the nutritional care of patients with Cystic Fibrosis. Curr. Opin. Clin. Nutr. Metab. Care 17, 515–520.

Escobedo Monge, M.F., Barrado, E., Alonso Vicente, C., Redondo del Río, M.P., Manuel Marugán de Miguelsanz, J., 2019. Zinc nutritional status in patients with cystic fibrosis. Nutrients 11, 150.

Farrell, P.M., Rosenstein, B.J., White, T.B., Accurso, F.J., Castellani, C., Cutting, G.R., Durie, P.R., LeGrys, V.A., Massie, J., Parad, R.B., Rock, M.J., Campbell, P.W., 2008. Guidelines for diagnosis of cystic fibrosis in newborns through older adults: cystic fibrosis foundation consensus report. J. Pediatr. 153, S4–S14.

Gao, W., Emaminejad, S., Nyein, H.Y.Y., Challa, S., Chen, K., Peck, A., Fahad, H.M., Ota, H., Shiraki, H., Kiriya, D., 2016. Fully integrated wearable sensor arrays for multiplexed in situ perspiration analysis. Nature 529, 509.

Gx Sweat Patch, n.d. . Epicore Biosystems.

Hirayama, T., Nagasawa, H., 2017. Chemical tools for detecting Fe ions. J. Clin. Biochem. Nutr. 60, 39–48.

Honari, G., Maibach, H., 2014. Chapter 1 - skin structure and function. In: Maibach, H., Honari, G. (Eds.), Applied Dermatotoxicology. Academic Press, Boston, pp. 1–10.

Kim, J., Jeerapan, I., Imani, S., Cho, T.N., Bandodkar, A., Cinti, S., Mercier, P.P., Wang, J., 2016. Noninvasive alcohol monitoring using a wearable tattoo-based iontophoretic-biosensing system. ACS Sens. 1, 1011–1019.

Kim, J., Wu, Y., Luan, H., Yang, D.S., Cho, D., Kwak, S.S., Liu, S., Ryu, H., Ghaffari, R., Rogers, J.A., 2022. A skin-interfaced, miniaturized microfluidic analysis and delivery system for colorimetric measurements of nutrients in sweat and supply of vitamins through the skin. Adv. Sci. 9, 2103331.

Kim, S.B., Koo, J., Yoon, J., Hourlier-Fargette, A., Lee, B., Chen, S., Jo, S., Choi, J., Oh, Y. S., Lee, G., Won, S.M., Aranyosi, A.J., Lee, S.P., Model, J.B., Braun, P.V., Ghaffari, R., Park, C., Rogers, J.A., 2019. Soft, skin-interfaced microfluidic systems with integrated enzymatic assays for measuring the concentration of ammonia and ethanol in sweat. Lab Chip 20, 84–92.

Koh, A., Kang, D., Xue, Y., Lee, S., Pielak, R.M., Kim, J., Hwang, T., Min, S., Banks, A., Bastien, P., Manco, M.C., Wang, L., Ammann, K.R., Jang, K.-I., Won, P., Han, S., Ghaffari, R., Paik, U., Slepian, M.J., Balooch, G., Huang, Y., Rogers, J.A., 2016. A soft, wearable microfluidic device for the capture, storage, and colorimetric sensing of sweat. Sci. Transl. Med. 8, 366ra165-366ra165.

Krebs, N.F., Westcott, J.E., Arnold, T.D., Kluger, B.M., Accurso, F.J., Miller, L.V., Hambidge, K.M., 2000. Abnormalities in zinc homeostasis in young infants with cystic fibrosis. Pediatr. Res. 48, 256–261.

Lambers, H., Piessens, S., Bloem, A., Pronk, H., Finkel, P., 2006. Natural skin surface pH is on average below 5, which is beneficial for its resident flora. Int. J. Cosmet. Sci. 28, 359–370.

Lee, D.H., Lim, S., Kwak, S.S., Kim, J., 2023. Advancements in skin-mediated drug delivery: mechanisms, techniques, and applications. https://onlinelibrary.wiley.com/doi/10.1002/adhm.202302375, 12.15.23.

Lyczak, J.B., Cannon, C.L., Pier, G.B., 2002. Lung infections associated with cystic fibrosis. Clin. Microbiol. Rev. 15, 194–222.

Min, J., Demchyshyn, S., Sempionatto, J.R., Song, Y., Hailegnaw, B., Xu, C., Yang, Y., Solomon, S., Putz, C., Lehner, L.E., Schwarz, J.F., Schwarzinger, C., Scharber, M.C., Shirzaei Sani, E., Kaltenbrunner, M., Gao, W., 2023. An autonomous wearable biosensor powered by a perovskite solar cell. Nat Electron 6, 630–641.

Moritz, A.R., Henriques, F.C., 1947. Studies of thermal injury. Am. J. Pathol. 23, 695–720.

Ooi, C.Y., Durie, P.R., 2016. Cystic fibrosis from the gastroenterologist's perspective. Nat. Rev. Gastroenterol. Hepatol. 13, 175–185.

Radiation: Electromagnetic fields [WWW Document], n.d. URL https://www.who.int/news-room/questions-and-answers/item/radiation-electromagnetic-fields (accessed 10.12.23).

Ray, T.R., Ivanovic, M., Curtis, P.M., Franklin, D., Guventurk, K., Jeang, W.J., Chafetz, J., Gaertner, H., Young, G., Rebollo, S., Model, J.B., Lee, S.P., Ciraldo, J., Reeder, J.T., Hourlier-Fargette, A., Bandodkar, A.J., Choi, J., Aranyosi, A.J., Ghaffari, R., McColley, S.A., Haymond, S., Rogers, J.A., 2021. Soft, skin-interfaced sweat stickers for cystic fibrosis diagnosis and management. Sci. Transl. Med. 13, eabd8109.

Reeder, J.T., Choi, J., Xue, Y., Gutruf, P., Hanson, J., Liu, M., Ray, T., Bandodkar, A.J., Avila, R., Xia, W., Krishnan, S., Xu, S., Barnes, K., Pahnke, M., Ghaffari, R., Huang, Y., Rogers, J.A., 2019. Waterproof, electronics-enabled, epidermal microfluidic devices for sweat collection, biomarker analysis, and thermography in aquatic settings. Sci. Adv. 5, eaau6356.

Ruzal-Shapiro, C., 1998. Cystic fibrosis: an overview. Radiol. Clin. 36, 143–161.

Sempionatto, J.R., Lin, M., Yin, L., De la paz, E., Pei, K., Sonsa-ard, T., de Loyola Silva, A. N., Khorshed, A.A., Zhang, F., Tostado, N., Xu, S., Wang, J., 2021. An epidermal patch for the simultaneous monitoring of haemodynamic and metabolic biomarkers. Nat. Biomed. Eng. 5, 737–748.

Tashiro, G., Wada, M., Sakurai, M., 1961. A bromphenol blue method for visualizing sweat at the openings of the sweat Ducts**From the physiological laboratory, Tohoku University School of medicine, Sendai, Japan. J. Invest. Dermatol. 36, 3–4.

Tu, J., Min, J., Song, Y., Xu, C., Li, J., Moore, J., Hanson, J., Hu, E., Parimon, T., Wang, T.-Y., Davoodi, E., Chou, T.-F., Chen, P., Hsu, J.J., Rossiter, H.B., Gao, W., 2023. A wireless patch for the monitoring of C-reactive protein in sweat. Nat. Biomed. Eng. 7, 1293–1306.

Van Biervliet, S., Van Biervliet, J.P., Vande Velde, S., Robberecht, E., 2007. Serum zinc concentrations in cystic fibrosis patients aged above 4 Years: a cross-sectional evaluation. Biol. Trace Elem. Res. 119, 19–26.

Wang, J., Niu, Y., Zhang, C., Chen, Y., 2018. A micro-plate colorimetric assay for rapid determination of trace zinc in animal feed, pet food and drinking water by ion masking and statistical partitioning correction. Food Chem. 245, 337–345.

Wang, M., Yang, Y., Min, J., Song, Y., Tu, J., Mukasa, D., Ye, C., Xu, C., Heflin, N., McCune, J.S., Hsiai, T.K., Li, Z., Gao, W., 2022. A wearable electrochemical biosensor for the monitoring of metabolites and nutrients. Nat. Biomed. Eng. 6, 1225–1235.

Zhang, Y., Guo, H., Kim, S.B., Wu, Y., Ostojich, D., Park, S.H., Wang, X., Weng, Z., Li, R., Bandodkar, A.J., Sekine, Y., Choi, J., Xu, S., Quaggin, S., Ghaffari, R., Rogers, J.A., 2019. Passive sweat collection and colorimetric analysis of biomarkers relevant to kidney disorders using a soft microfluidic system. Lab Chip 19, 1545–1555.